

# **Computation of Stress Intensity Factors**

## **Using MSC/PROBE Version 5**

John E. Schiermeier  
Senior Development Engineer

The MacNeal-Schwendler Corporation  
Los Angeles, California

Presented at  
The 1993 MSC World Users' Conference

### **Abstract**

In fracture mechanics, the stress intensity factor is used to determine whether a crack will run, possibly causing catastrophic failure, or arrest. Typically this value can be computed from the stress or displacement fields around the crack tip, either by hand or by numerical methods, and then compared with empirical data.

MSC/PROBE-PLANAR has long had two methods of computing Mode I and II stress intensity factors which take advantage of the p-version, the contour integral and cutoff function methods, as well as the standard energy release rate. In Version 5, MSC/PROBE-SOLID has incorporated singularity elements to model exactly the displacement field for a closed crack, and the crack-opening displacement (COD) method to automatically compute Mode I, II, and III stress intensity factors. Combined with the automatic p-adaptivity, accurate and reliable factors may be computed for fully three-dimensional problems in an efficient manner.

This paper provides an explanation of the stress intensity factors and the methods used to compute them. Sample problems are run, using MSC/XL V3B as the pre- and post-processor, and the computed stress intensity factors are compared with theoretical results where available.

## **1. Introduction**

### **1.1. p-Version of the Finite Element Method**

In the p-version of the finite element method, the number of shape functions for each element can be increased to include polynomials of higher degree, as described in reference [1]. In this case, the error of approximation is controlled not only by mesh refinement, but also by increasing the polynomial degree of elements.

The p-version is useful for problems where the detailed stress state is of importance. Fracture mechanics problems tend to fall into this category; the engineer is interested in determining the precise stress state around the crack tip, so that the stress intensity factor can be computed to determine whether the part must be replaced. Given the continuous nature of the p-version solution, which approximates the theory of elasticity instead of the mechanics of materials, specialized methods have been developed to calculate stress intensity factors [1]. Some of these methods have been implemented in MSC/PROBE.

### **1.2. p-Version Quality Control Procedures**

After the p-version analysis has been performed, the quality and reliability of the final solution must still be assessed. This evaluation involves three quality control procedures within MSC/PROBE:

1. Relative error in energy norm;
2. Equilibrium of elements and inter-element continuity;
3. Continuity and convergence of point functionals.

The first criterion, using the global energy, is based on theoretical convergence rates and serves as a global error estimator. An estimated strain energy is calculated from the sequence of solutions, and then the error is computed. The second criterion uses an element error indicator that reliably combines the equilibrium and continuity information into one quantity. These should be lower in the areas of interest and decrease as the p-level increases. The third criterion, based on information at specified points, uses the expertise of the design engineer to determine the quantities of interest in the problem. In this case, the quantities of interest are the stress intensity factors. The convergence of those quantities should be evident as the p-level increases.

## 2. Fracture Mechanics

The geometry for a closed crack in a two-dimensional section is defined in Figure 1.

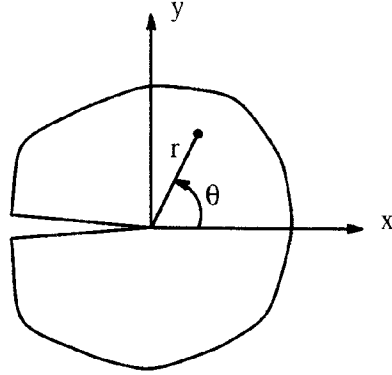


Figure 1. Crack Geometry.

In linear elastic fracture mechanics, there are three modes of fracture that can be considered. The first mode is called the opening mode, where the displacements in the y direction are symmetric about the x axis. The second mode is the shearing mode, where the displacements in the x direction are anti-symmetric about the x axis. The third mode is the tearing mode, where the displacements in the z direction are anti-symmetric about the x-axis.

The stress field near the crack tip may be derived from the Airy stress function in the biharmonic equation with the appropriate boundary conditions [1]. For Mode I the components are given by [2]:

$$\begin{aligned}\sigma_x &= \frac{K_I}{(2\pi r)^{1/2}} \cos \frac{\theta}{2} \left( 1 - \sin \frac{\theta}{2} \sin \frac{3\theta}{2} \right) \\ \sigma_y &= \frac{K_I}{(2\pi r)^{1/2}} \cos \frac{\theta}{2} \left( 1 + \sin \frac{\theta}{2} \sin \frac{3\theta}{2} \right) \\ \tau_{xy} &= \frac{K_I}{(2\pi r)^{1/2}} \sin \frac{\theta}{2} \cos \frac{\theta}{2} \cos \frac{3\theta}{2} .\end{aligned}\tag{1}$$

The stress fields for Modes II and III are similar. All three components of stress vary as  $1/r^{1/2}$ , which leads to an infinite stress at the crack tip. From an analysis standpoint, this is not very useful information; however, the term  $K_I$  is a constant. This term is called the stress intensity factor, or the coefficient of the singularity in mathematical terms, and can be compared with empirical data to determine whether the crack will run, which may often lead to catastrophic failure, or arrest.

The goal of a typical finite element analysis for a fracture model is then to determine the stress intensity factors  $K_I$ ,  $K_{II}$ , and/or  $K_{III}$  corresponding to the theoretical stress fields at the crack tip.

### 3. Computation of Stress Intensity Factors

There are many methods of computing the stress intensity factors  $K$  from a finite element solution. The next sections will describe four that are used in MSC/PROBE. MSC/PROBE-PLANAR uses the contour integral and cutoff function methods, which compute generalized stress intensity factors, and the energy release rate, which computes a combined stress intensity factor. MSC/PROBE-SOLID uses the crack-opening displacement method.

#### 3.1. Generalized Stress Intensity Factors

A more general form of the displacement field  $\{u\}$  around the crack tip is given by:

$$\{u\} = \sum_{i=1}^{\infty} \frac{A_i^1}{2G} r^{\lambda_i^1} \{f_i^1(\theta)\} + \sum_{i=1}^{\infty} \frac{A_i^2}{2G} r^{\lambda_i^2} \{f_i^2(\theta)\}, \quad (2)$$

where  $A_i^1$  and  $A_i^2$  are the generalized stress intensity factors for Modes I and II, respectively, and  $\lambda_i^1$  and  $\lambda_i^2$  are the strengths of the singularity, which depend only on the geometry for the homogeneous isotropic case [1]. The functions  $f_i$  are some general functions of only  $\theta$ . For a closed crack,  $\lambda_1^1 = \lambda_1^2 = 1/2$ ; therefore,  $A_1^1 = K_I/(2\pi)^{1/2}$  and  $A_1^2 = K_{II}/(2\pi)^{1/2}$ , giving the same form as equations (1). The form (2) is more general, in that it applies to any crack opening geometry and includes the higher-order terms.

##### 3.1.1. Contour Integral Method

The first method for computing the generalized stress intensity factors  $A_j^m$ , where  $j$  is the term and  $m$  is the mode, is called the contour integral method [1]. This method uses the concept of an extraction function,  $\{w_j^m\}$ , which is similar to a single term of  $\{u\}$  but has a  $-\lambda_j^m$  strength of singularity. Given the traction vector  $\{T^u\}$  corresponding to solution  $\{u\}$ , the factors are given by:

$$A_j^m = \int_{\Gamma} ([w_j^m] \{T^u\}) ds - \int_{\Gamma} ([u] \{T^w\}) ds \quad (3)$$

on any counter-clockwise path  $\Gamma$  from one crack face to the other. The finite element solution for  $\{u\}$  and  $\{T^u\}$  is substituted for the exact solution in order to compute the factors. This method separates the Mode I and Mode II stress intensity factors, and converges very quickly, on the order of the energy, since an extraction function is used.

In MSC/PROBE-PLANAR, the engineer specifies a path of element edges leading from one crack face to the other for the integration to be performed. Having the path consist of element edges is a convenience, not a necessity; the path could go through the interior of elements just as easily, which would have the added advantage avoiding stress discontinuities between elements. It is recommended that the engineer have two layers of elements around the crack tip, and specify the outer boundary for the contour.

The contour integral method was extended to the case of two-dimensional bi-material anisotropic wedges in reference [3], using the two Lekhnitskii stress functions instead of the single Airy stress function.

This method should be distinguished from the J integral, which is another contour integral used to calculate stress intensity factors:

$$J = \int_{\Gamma} \left( w \, dy - T_i \frac{\partial u_i}{\partial x} \, ds \right) \quad (4)$$

$$w = \int_0^{\epsilon_{ij}} \sigma_{ij} \, d\epsilon_{ij} ,$$

where  $w$  is the strain energy density [4]. This integral has applications in elastic/plastic fracture mechanics, and does not use the concept of an extraction function. For elastic conditions, the value of  $J$  is equal to the energy release rate described below.

### 3.1.2. Cutoff Function Method

The second method for computing the generalized stress intensity factors is the cutoff function method [1]. This method uses the same extraction function  $\{w_j^m\}$  as the contour integral method, but multiplies it by a cutoff function dependent on  $r$  to modify the behavior in different parts of the domain  $\Omega$ . The generalized stress intensity factors are then given by:

$$A_j^m = \int_{\Gamma_3} (T_n^w u_n + T_t^w u_t) \, ds - \int_{\Gamma_4} (T_n^w u_n + T_t^w u_t) \, ds \quad (5)$$

$$+ \iint_{\Omega} \left[ \left( \frac{\partial \sigma_x^w}{\partial x} + \frac{\partial \tau_{xy}^w}{\partial y} \right) u_x + \left( \frac{\partial \tau_{xy}^w}{\partial x} + \frac{\partial \sigma_y^w}{\partial y} \right) u_y \right] dx \, dy ,$$

where the subscripts  $n$  and  $t$  refer to the normal and tangent directions, respectively. The domain  $\Omega$  is bounded by two circles around the crack tip,  $\Gamma_1$  and  $\Gamma_2$ , and the two segments on the crack face,  $\Gamma_3$  and  $\Gamma_4$ , and must be evaluated in counter-clockwise order. With the addition of the cutoff function to the extraction function, the results are generally more accurate than the contour integral method. The cutoff function method also separates the Mode I and Mode II stress intensity factors, and converges very quickly, on the order of the energy, since an extraction function is used.

In MSC/PROBE-PLANAR, the engineer must have two circular layers of elements around the crack tip, because of the specific cutoff function used, and specify the outer layer of elements for the area integration.

### 3.2. Energy Release Rate

The energy release rate is a relatively simple way to compute the combined stress intensity factor. Given the definition of the energy release rate:

$$\mathcal{G} = - \frac{\partial \Pi}{\partial A} = \frac{1 - \nu^2}{E} K^2 \quad (6)$$

for the plane strain case, the potential energy  $\Pi$  and its derivative with respect to crack area  $A$  are given by:

$$\Pi = \frac{1}{2} [u][k]\{u\} - [f]\{u\} \quad (7)$$

$$\frac{\partial \Pi}{\partial A} = \left[ \frac{\partial u}{\partial A} \right] ([k]\{u\} - \{f\}) + \frac{1}{2} [u] \left[ \frac{\partial k}{\partial A} \right] \{u\} - [u] \left\{ \frac{\partial f}{\partial A} \right\} ,$$

where  $[k]$  is the stiffness matrix,  $\{f\}$  is the load vector,  $\{u\}$  is the solution vector, and assuming that  $[k]$  is symmetric for the scalar triple product [5]. Since the expression in parentheses is defined to

be zero by the finite element solution, the following expression remains:

$$K^2 = - \frac{E}{1-\nu^2} \left( \frac{1}{2} [u] \left[ \frac{\partial k}{\partial A} \right] \{u\} + [u] \left\{ \frac{\partial f}{\partial A} \right\} \right) . \quad (8)$$

The stiffness and force derivatives may be computed by finite differences. It is not necessary to perform another linear equation solution for the crack extension. The stiffness matrices and load vectors for only the elements adjacent to the crack tip will change, so that the computational requirements are not great. Unlike the contour integral and cutoff function methods, the energy release rate does not separate the Mode I and Mode II stress intensity factors for mixed-mode loading, but it still converges quickly.

### 3.3. Singularity Elements

One type of singularity element contains the singularity in the mapping of the jacobian. This can be most easily demonstrated in one dimension, as shown in Figure 2.

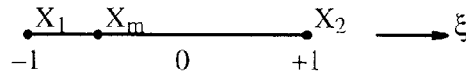


Figure 2. One-Dimensional Singularity Element.

For a one-dimensional isoparametric element, the mapping and Jacobian are given by:

$$\begin{aligned} x &= -\xi \left( \frac{1-\xi}{2} \right) X_1 + \xi \left( \frac{1+\xi}{2} \right) X_2 + (1-\xi^2) X_m \\ \frac{\partial x}{\partial \xi} &= -\left( \frac{1}{2} - \xi \right) X_1 + \left( \frac{1}{2} + \xi \right) X_2 + (-2\xi) X_m . \end{aligned} \quad (9)$$

If the midpoint is located at the quarter point, as shown in Figure 2, the mapping is given by:

$$\begin{aligned} X_m &= \frac{3}{4} X_1 + \frac{1}{4} X_2 \\ \frac{\partial x}{\partial \xi} &= -\left( \frac{1}{2} + \frac{1}{2}\xi \right) X_1 + \left( \frac{1}{2} + \frac{1}{2}\xi \right) X_2 \\ &= \frac{1}{2} (X_2 - X_1) (1 + \xi) . \end{aligned} \quad (10)$$

At  $\xi=-1$ , the jacobian is zero. Since the inverse of the jacobian is used to compute the strains and stresses, there is a singularity in those fields at the specified point. In this case, since the jacobian is linear, the singularity is of the form  $1/r$ .

For triangular elements, the singularity is of the form  $1/r^{1/2}$  at one of the vertices when the midside nodes on the two adjacent edges are at the quarter points [6]. This singularity matches the singularity in equations (1). A pentahedral element is the extension of the triangular element, having the same singularity along one of the three vertical edges when the four adjacent midside nodes are at the quarter points. For a tetrahedral element, the singularity is at one of the vertices when the three adjacent midsides are at the quarter points. Quadrilateral and hexahedral elements only have the singularity behavior along the edges, not over the interior, and therefore are not as useful.

### 3.4. Crack–Opening Displacement Method

The expressions for the displacements at  $\theta=\pi$  in terms of the stress intensity factors for the three modes of fracture are given by:

$$\begin{aligned} v &= \frac{K_I}{G} [r/(2\pi)]^{1/2} 2(1 - \nu) \\ u &= \frac{K_{II}}{G} [r/(2\pi)]^{1/2} 2(1 - \nu) \\ w &= \frac{K_{III}}{G} [(2r)/\pi]^{1/2} \end{aligned} \quad (11)$$

for the case of plane strain [2]. For the case of plane stress,  $\nu$  can be replaced by  $\nu/(1+\nu)$ . The stress intensity factors are then given by:

$$\begin{aligned} K_I &= \frac{E}{4(1 - \nu^2)} [(2\pi)/r]^{1/2} v \\ K_{II} &= \frac{E}{4(1 - \nu^2)} [(2\pi)/r]^{1/2} u \\ K_{III} &= \frac{E}{2(1 + \nu)} [\pi/(2r)]^{1/2} w \end{aligned} \quad (12)$$

for plane strain, where the isotropic material relation for  $G$  has been used. For plane strain, the  $(1-\nu^2)$  term is omitted in the first two relations.

The displacements are used instead of the stresses in the calculation of the stress intensity factors for several reasons. They are finite at the crack tip, continuous across element boundaries, and converge faster than the stresses. Even though the displacements are finite at the crack tip, the expressions (12) can not be used because of the  $r$  in the denominator. The expressions (12) at the crack tip have an indeterminate form, which has a limit, but errors in the finite element solution could be magnified at the singularity. Consequently, the displacements used must be a small distance away from the crack tip, so that the expressions are valid, but not so far that higher–order terms have a significant influence.

There is also the issue of plane stress or plane strain conditions in equations (12) when dealing with a three–dimensional analysis. If the crack tip is on a free surface, then plane stress can be used; if it is in the middle, where symmetry often occurs, then plane strain can be used. However, the real situation is often between these two cases, and so computing the  $K$  values for each case can provide lower and upper bounds.

## 4. Sample Problems

Four sample fracture mechanics problems are considered. The first two, a cracked strip and a cracked disk, are simple two-dimensional problems that are analyzed in both MSC/PROBE-PLANAR and MSC/PROBE-SOLID V5 [7], so that solutions for all the methods may be compared to handbook values. The third problem, a cracked tube, is a three-dimensional problem and is compared to handbook values. The fourth problem, a cracked splicing fixture, is a more realistic problem and does not have a handbook value.

Other sample fracture mechanics problems with MSC/PROBE are given in reference [8].

### 4.1. Center-Cracked Strip

The center-cracked strip under uniaxial tension is a standard benchmark test for fracture mechanics. It was analyzed with both MSC/PROBE-PLANAR, using 28 elements, and MSC/PROBE-SOLID, using ten. The planar mesh had to use no symmetry and two rings of elements around the crack tip for the fracture methods discussed earlier. The solid mesh used symmetry and four singularity elements around the crack tip instead of the two rings. The deformed shape of the solid mesh is shown in Figure 3. A value of  $q=1$  was used for the transverse polynomial degree, but the solution is still different from the planar solution because of the non-zero Poisson's ratio.

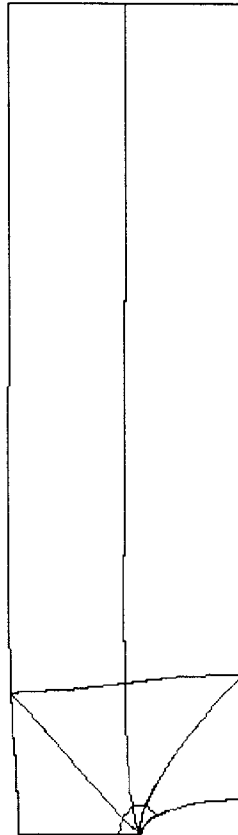


Figure 3. Center-Cracked Strip.



In Figure 4, the first two steps of the quality control procedures are presented, as discussed earlier. The error in energy norm is shown on a log-log plot versus the number of degrees of freedom. The constant slope for  $p=3$  and higher indicates that the solution is dominated by the singularity, the strength of which can be calculated from the slope [1]. The error indicators are shown by color-coding the elements. The elements with the least error are the large two on top, which carry the load into the area of the crack. The two on the left, which comprise the ligament, have a worse error, and the two on the right, which are close to the crack face, have the worst error. The error is highest there because the stress must meet the free surface conditions on the crack face. Since the error indicators are based on the stress, they are difficult to interpret for the singularity elements.

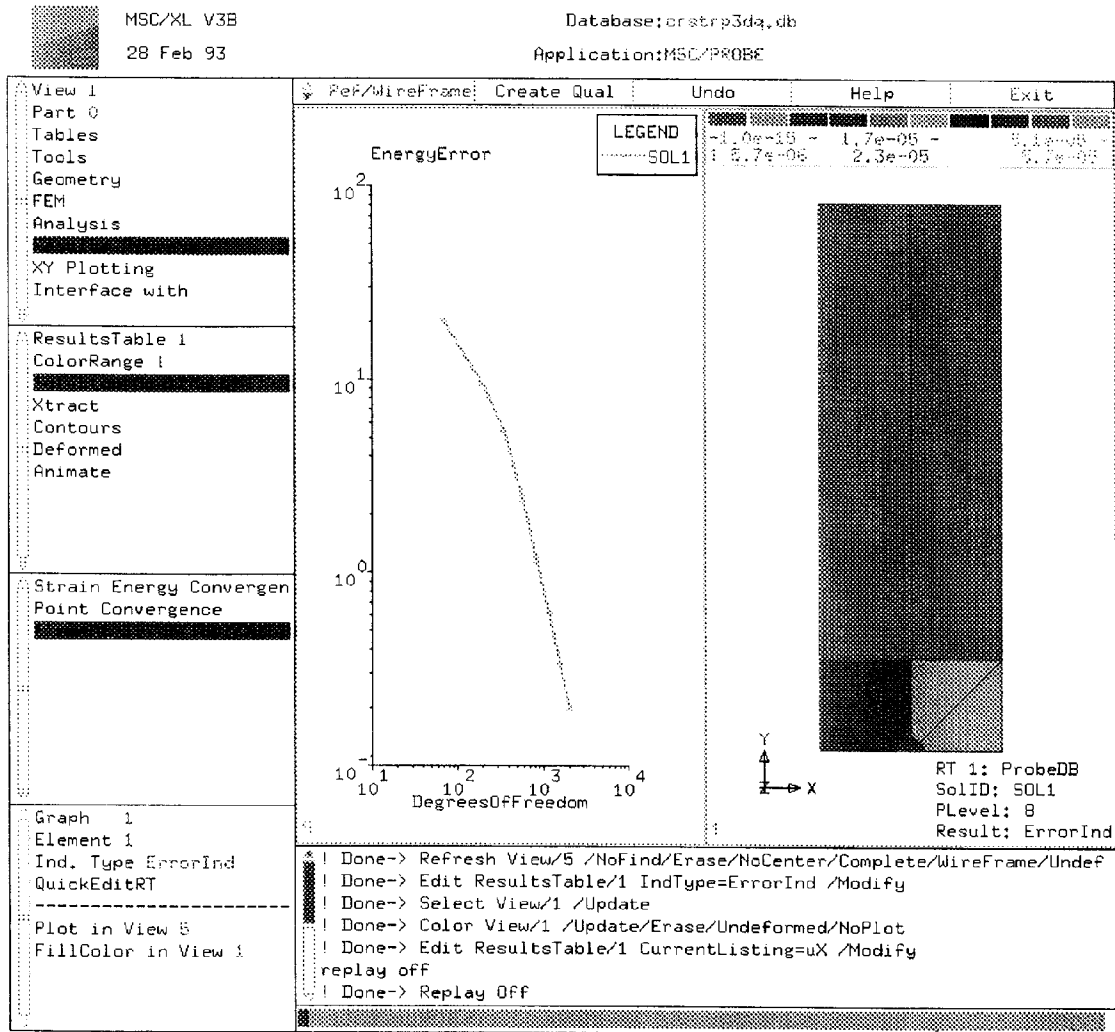


Figure 4. Relative Error in Energy Norm and Element Error Indicators.

The convergence of the stress intensity factors for both models and all four methods is listed in Table 1. These can be compared with the theoretical  $K_I$  of 1.487 [2]. The cutoff function method, which is the most accurate of the planar methods, is exact to four digits, and the other two methods differ by less than 0.1%. For the crack-opening displacement method, the values of the stress inten-

sity at the edge and in the center give bounds on the three-dimensional distribution, and the two-dimensional value is approximately the average. It would be possible to have a constant distribution by setting the Poisson's ratio to zero, but this would trivialize the problem.

Table 1. Center-Cracked Strip.  
(Theoretical  $K_I=1.487$ .)

p-level	MSC/PROBE-PLANAR			MSC/PROBE-SOLID	
	contour int.	cutoff func.	ERR	COD, edge	COD, center
1	1.835	1.455	1.542	1.321	1.452
2	1.384	1.518	1.504	1.440	1.583
3	1.535	1.484	1.477	1.399	1.538
4	1.467	1.488	1.482	1.414	1.554
5	1.496	1.487	1.482	1.419	1.560
6	1.483	1.487	1.484	1.422	1.562
7	1.489	1.487	1.484	1.422	1.563
8	1.486	1.487	1.485	1.422	1.563

The solid model could be expanded to include ribs, stiffeners, curvature, or other details to become a more realistic model.

#### 4.2. Cracked Disk

The rotating cracked disk is another planar problem for which theoretical solutions exist. It was analyzed in MSC/PROBE-PLANAR, using 38 elements, and MSC/PROBE-SOLID, using 15. The planar mesh used no symmetry and two rings of elements around the crack tip. The solid mesh used symmetry and 15 elements, with four singularity elements around the crack tip instead of the two rings. The deformed solid mesh is shown in Figure 5. The planar mesh used plane stress conditions, and the solid mesh used  $\nu=1$  with the non-zero Poisson's ratio.

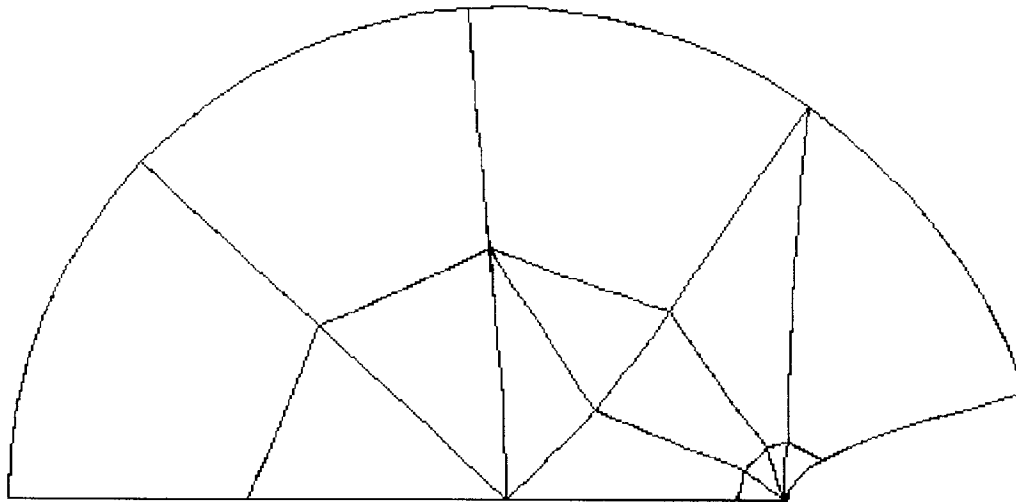


Figure 5. Cracked Disk.

Contours of the maximum principal stress for the cracked disk are shown in Figure 6. On the left side, the crack does not have much influence, so the contours are concentric. On the right side, there is a sharp gradient where the stresses must meet the free surface conditions on the crack face. Since the stresses are infinite at the crack tip, contours can not be drawn on the singularity elements.

The convergence of the stress intensity factors for both models and all four methods is listed in Table 2. These can be compared with the theoretical  $K_I$  of 27.75 for plane stress and 26.68 for plane strain [2]. (Note that there is an error in reference [2] which was confirmed by its author.) The three planar methods are within 2%; however, in order to compute the theoretical solutions, two constants had to be used. One of these constants was read from a graph with a given accuracy of 2%, so the theoretical solution should not be assumed to be better than that. The edge and center values for the solid solution again bound the theoretical answer, with the average close to the plane stress solution.

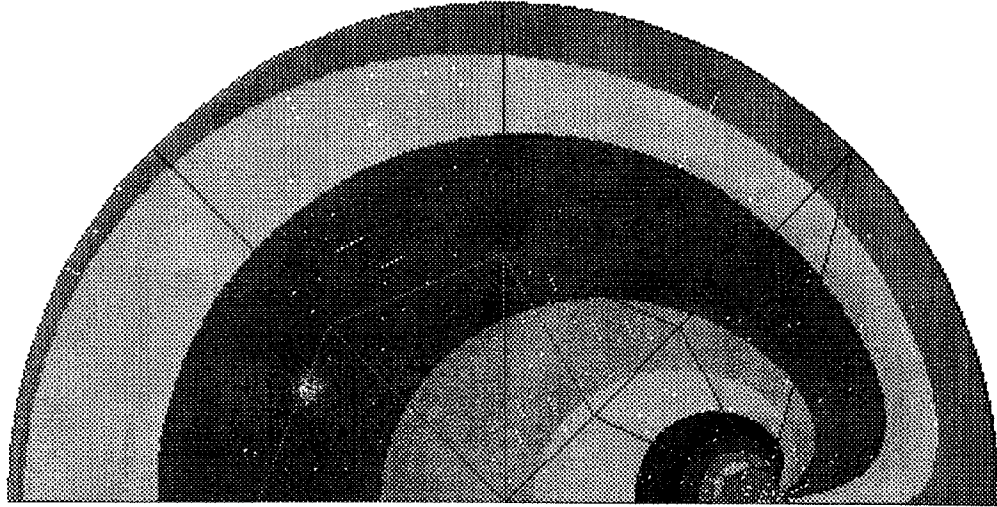


Figure 6. Contours of Maximum Principal Stress.

Table 2. Cracked Disk.  
(Theoretical  $K_I=27.75$ , plane stress; 26.68, plane strain.)

p-level	MSC/PROBE-PLANAR			MSC/PROBE-SOLID	
	contour int.	cutoff func.	ERR	COD, edge	COD, center
1	31.08	24.83	26.36	23.96	26.32
2	24.94	27.79	27.64	26.55	29.17
3	28.17	27.36	27.30	25.76	28.31
4	26.82	27.30	27.27	25.96	28.52
5	27.40	27.31	27.31	26.10	28.68
6	27.16	27.32	27.33	26.18	28.76
7	27.27	27.32	27.34	26.23	28.82
8	27.22	27.32	27.35	26.25	28.85

The solid model could be modified to include additional features, such as blades of a propeller or turbine, and become a more practical problem.

### 4.3. Cracked Tube

The cracked tube is a three-dimensional problem for which theoretical solutions exist. It was analyzed in MSC/PROBE-SOLID, using symmetry and 18 elements with four singularity elements around the crack tip. The crack is in the circumferential direction. (Solutions also exist for a crack in the axial direction.) The deformed shape is shown in Figure 7 for the tension case. Tension, moment, and torsion load cases were analyzed, and a value of  $q=1$  was used.

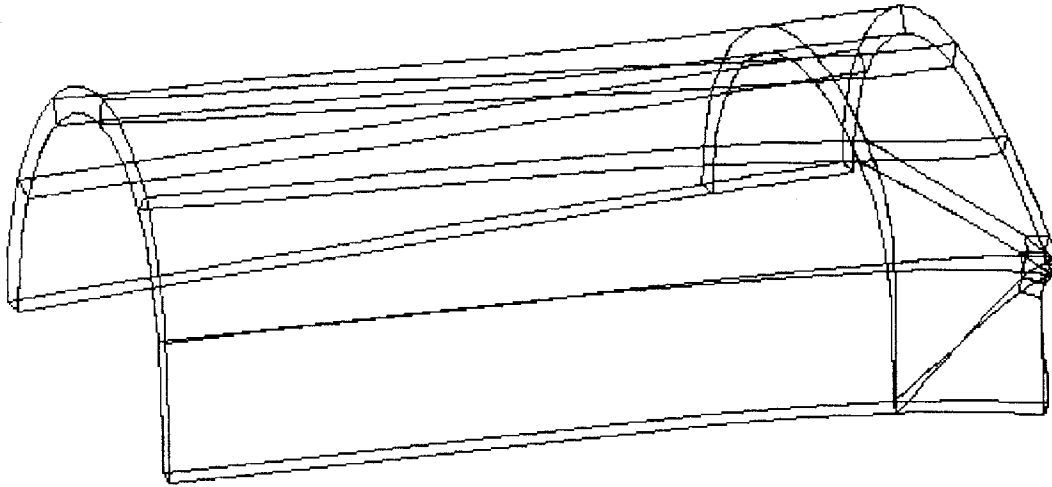


Figure 7. Cracked Tube (tension).

Contours of the maximum principal stress for the cracked tube are shown in Figure 8 for the tension case. Without the crack, the stress field would be uniform. The plot shows the perturbation of the stress field by the crack. Since the stresses are infinite at the crack tip, contours can not be drawn on the singularity elements.

The convergence of the stress intensity factors for the three load cases at the center is listed in Table 3. These can be compared with the theoretical  $K_I$  of 2545 for tension and 4784 for the moment case [2]. Reference [2] did not have a solution for the torsion case. The values converge strongly to 2779 and 5144 at the center point, significantly above the theoretical values; however, on the inner edge they converge to 2363 and 4321. The averages of these two values are about 1% different from the theoretical values, which demonstrates that the plane stress and plane strain assumptions provide bounds for the three-dimensional solution. The torsion  $K_{II}$  and  $K_{III}$  converge strongly to 2433 and 1234, respectively, indicating that the shearing mode is worse than the tearing mode.



Figure 8. Contours of Maximum Principal Stress (tension).

Table 3. Cracked Tube.  
(Theoretical  $K_I=2545$ , tension; 4784, moment.)

p-level	Stress Intensity Factor at Center			
	tension $K_I$	moment $K_I$	torsion $K_{II}$	torsion $K_{III}$
1	2033.	3569.	1405.	566.4
2	2666.	4899.	2424.	1209.
3	2634.	4871.	2353.	1118.
4	2725.	5043.	2401.	1202.
5	2761.	5111.	2423.	1228.
6	2774.	5134.	2432.	1234.
7	2778.	5142.	2434.	1235.
8	2779.	5144.	2433.	1234.

#### 4.4. Cracked Splicing Fixture

The splicing fixture is a model which has been used in previous MSC/PROBE studies [9,10]. One of the reasons for its repeated usage is that it is an industrial problem with a small number of elements. For this study, an elliptical crack was introduced on the front symmetry plane in the area of maximum principal stress. The original model had 18 elements, of which six were changed and 42 were added for the crack. The deformed shape with 60 elements is shown in Figure 9. Most of the added elements were necessary to transition the geometry of the crack around the hole and back to the border of the model. There are symmetry conditions on the front and left faces, a normal constraint on the top face, and a linearly varying normal load around the top of the hole to simulate a bolt being pulled through the hole.

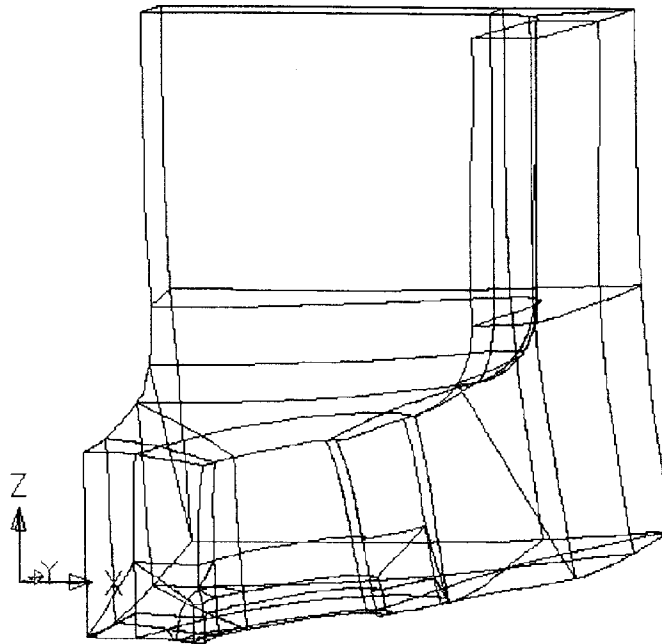


Figure 9. Cracked Splicing Fixture.

The detail of the mesh at the crack front is shown in Figure 10. Given the elliptical shape of the crack, three layers of elements were used to model the shape. Each of these three layers had four pentahedral singularity elements, for a total of twelve. Pentas were also used to transition the mesh away from the hole, as is seen in the figure, and around the hole to decrease the number of elements from eight per layer to five per layer. Even with the 60 elements, the singularity elements allow a coarse mesh around the crack. Automatic  $p$ -adaptivity was used for the problem [10], with the twelve singularity elements specified to increase with uniform  $p$ -level. The element  $p$ -levels determined by the adaptivity are shown in Figure 11. The highest adaptive  $p$ -levels were used in the elements in the fillets: the back fillet was highest, followed by the right fillet, and the vertical fillet. Most of the other elements remained at  $p=3$ , except for those at the crack tip specified to increase uniformly.

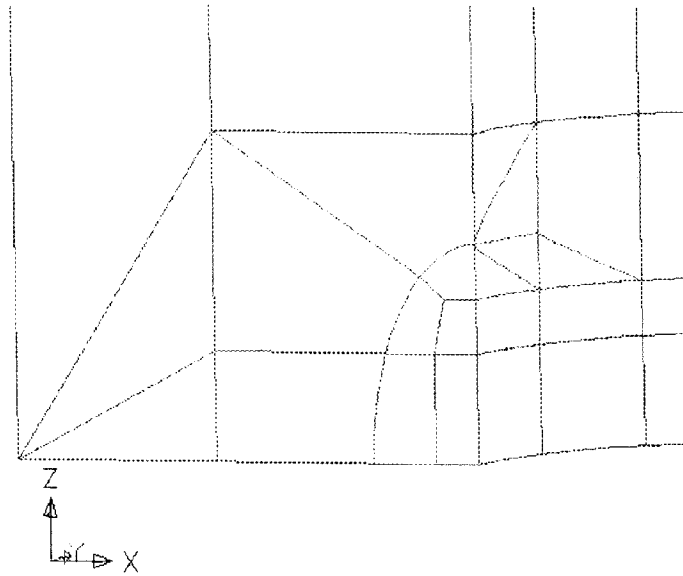


Figure 10. Mesh Detail at Crack Front.

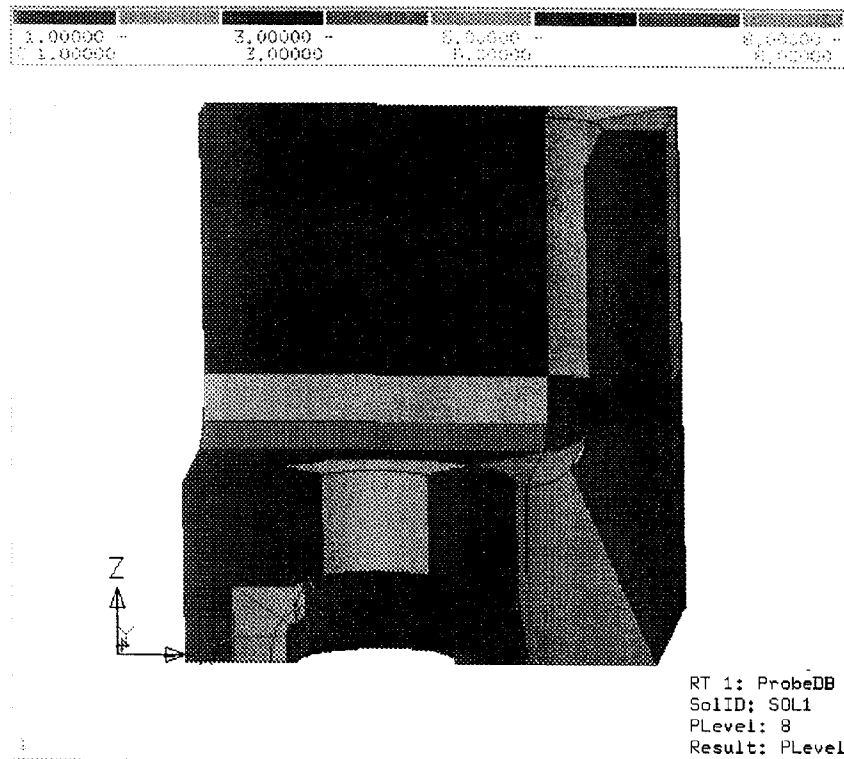


Figure 11. Element p-Levels.

Stress profiles for four locations around the crack front are shown in Figure 12. The four paths are numbered with their direction shown by arrows on the left, from the bottom to the top of the crack



front. The maximum principal stresses corresponding to these paths are plotted on the right. It can be seen that the highest stress occurs at the bottom, and the stress decreases around the crack front. Since the stresses at the crack tip are infinite in the singularity elements, they can not be numerically calculated and are plotted as zero. These profiles are useful to view the gradient leading into the crack tip and the values a short distance away. Such values could be compared with yield stresses to estimate the size of the plastic area around the crack tip. (Of course if yielding did occur, the stresses would be re-distributed, so that a nonlinear analysis would be appropriate.)

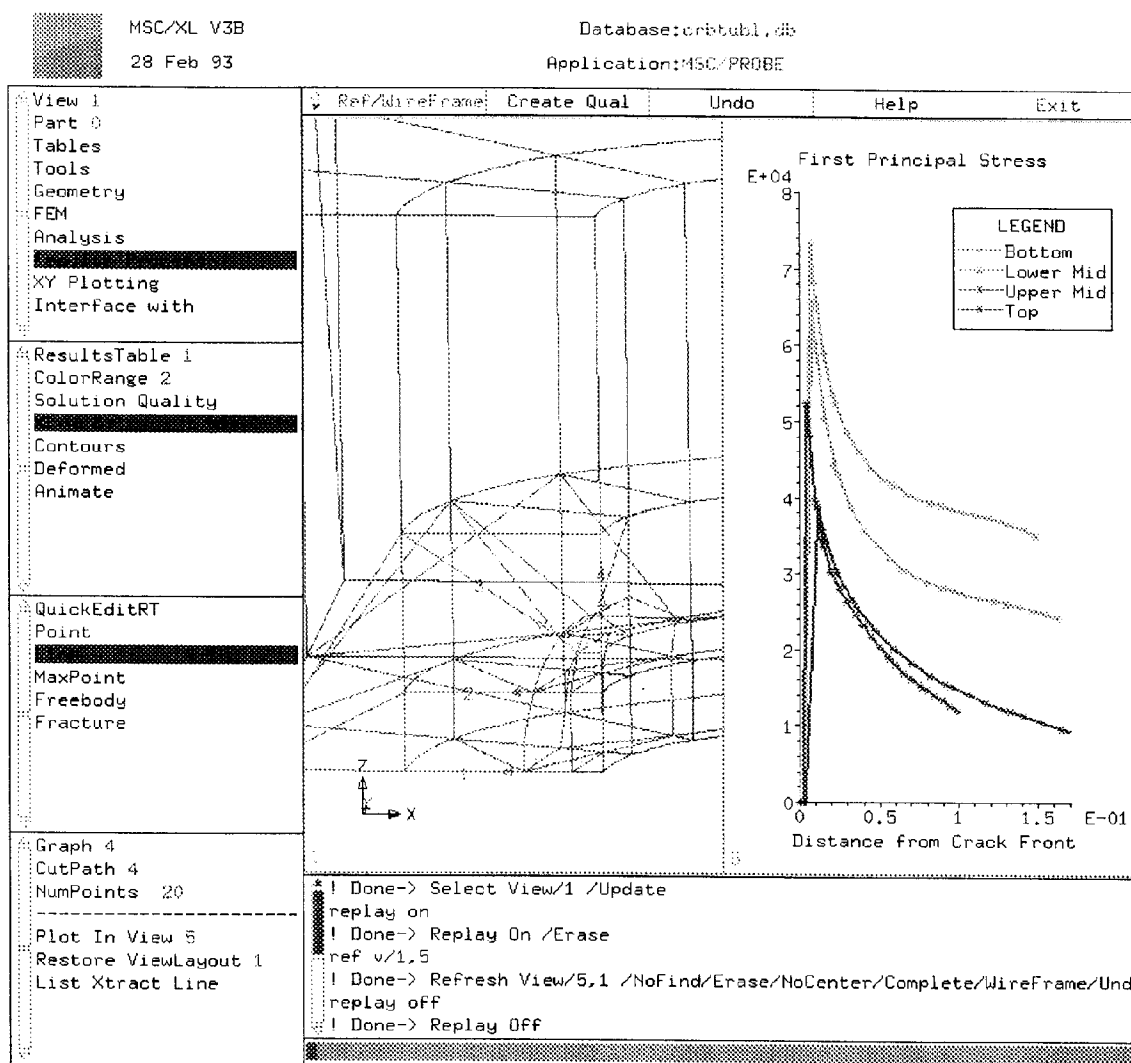


Figure 12. Stress Profiles at Crack Front.

The convergence of the stress intensity factor at the bottom, middle, and top of the elliptical crack is shown in Figure 13 and listed in Table 4. The middle value converges the best, with the bottom and top values converging more slowly in an ascending fashion. The critical value is at the bottom, as expected, so that the elliptical crack would tend to grow into a circular crack.

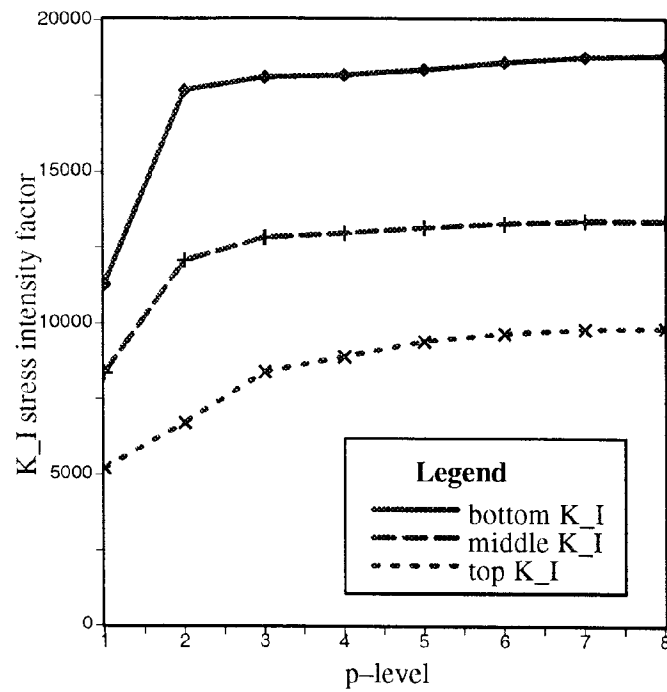


Figure 13. Convergence of Stress Intensity Factors for Cracked Splicing Fixture.

Table 4. Cracked Splicing Fixture.

p-level	Stress Intensity Factor		
	bottom K <sub>I</sub>	middle K <sub>I</sub>	top K <sub>I</sub>
1	11280.	8357.	5210.
2	17680.	12070.	6707.
3	18110.	12830.	8391.
4	18180.	12970.	8901.
5	18360.	13160.	9408.
6	18600.	13290.	9661.
7	18760.	13370.	9804.
8	18820.	13370.	9855.

These values can be compared with empirical values to determine if and then how fast the crack will grow. Given the coarse construction of the mesh, it would be relatively easy to modify the crack front and re-analyze the model to perform crack growth studies.

## 5. Summary and Conclusions

In this paper, stress intensity factors in general and the different methods of computing them in Version 5 of MSC/PROBE were presented. The contour integral and cutoff function methods, used to compute generalized stress intensity factors for any crack opening, and the energy release rate are implemented in MSC/PROBE-PLANAR. The singularity elements and the crack-opening displacement method are implemented in MSC/PROBE-SOLID. Four example problems were solved, ranging from standard benchmark problems to more practical problems.

Several of the methods take advantage of the p-version. The contour integral and cutoff function methods involve integrals of displacements and stresses over the domain, so that the continuous solution and ability to find results at any point of the domain are prerequisites. In addition, these methods converge on the order of the energy and separate the Mode I and Mode II stress intensity factors. The energy release rate does not separate the factors for mixed-mode loading.

The crack-opening displacement method requires accurate determination of displacements near the crack tip, which can be calculated anywhere within the p-version element. The displacements were used instead of the stresses because they are finite at the crack tip, continuous across element boundaries, and converge faster than the stresses. Singularity elements were added to decrease the number of elements required around the crack tip and therefore improve the efficiency of the analysis. Since these elements at the crack tip are larger, the displacements for the stress intensity calculation are calculated within the elements; these can be shown to be reliable values with the p-version.

After the p-version analysis has been performed, the quality and reliability of the final solution can be assessed, using the three quality control procedures within MSC/PROBE described earlier. First, the relative error in energy norm provides an estimate of the global error in the model. Second, the element error indicators show which elements in the model have the worst error. In addition, by observing the decrease of the indicators with increasing p-levels in the areas of interest, the indicators show that the added p-levels are reducing the error in the those areas. Finally, the convergence of the quantities of interest, in this case the stress intensity factors, as the p-level increases shows that they are accurate and reliable.

The stress intensity factors for the sample problems in MSC/PROBE converged very well and matched the theoretical cases. For the cracked strip and cracked disk, the planar results matched to within the accuracy of the reference, and the solid results matched to within the range for the plane stress and plane strain values. For the cracked tube, the solid results again matched the reference to within the range. For the cracked splicing fixture, there was no reference solution available, but the results were shown to converge as the p-level increased, demonstrating the accuracy of the solution.

The advantages of using the p-version to calculate stress intensity factors are evident. With the larger elements, especially the solid singularity elements, it is more convenient to mesh the crack with a graphical pre-processor such as MSC/XL V3B. The crack face can then be easily moved to perform crack growth studies, such as would be possible with the sample problems, without having to re-mesh the problem. The ability to perform multiple solutions on a single mesh, especially with the adaptivity in V5, and to view the convergence of results, provides an efficient and reliable way to calculate stress intensity factors for fracture mechanics problems.

## 6. References

1. Szabó, B.A. and Babuska, I., *Finite Element Analysis*, John Wiley & Sons, New York, 1991.
2. Tada, H., *The Stress Analysis of Cracks Handbook*, Second Edition, Paris Productions Inc., St. Louis, 1985.
3. Schiermeier, J.E., *Numerical Analysis of Stress Singularities in Composite Materials*, Master of Science Thesis, Washington University, St. Louis, May 1987.
4. Paris, P.C., *ME 520: Fracture Mechanics Class Notes*, Washington University, St. Louis, Fall 1987.
5. Parks, D.M., "A Stiffness Derivative Finite Element Technique for Determination of Crack Tip Stress Intensity Factors," *International Journal of Fracture*, Vol. 10, No. 4, December 1974, pp. 487–502.
6. Cook, R.D., *Concepts and Applications of Finite Element Analysis*, Second Edition, John Wiley & Sons, New York, 1981.
7. MSC/PROBE V5 User's Manuals, The MacNeal–Schwendler Corporation, 1991.
8. Heskitt, M.J., "MSC/PROBE Application Example: Planar, Axisymmetric, and Solid Fracture Mechanics," The MacNeal–Schwendler Corporation, 1990.
9. "MSC/PROBE Sample Problem: Splicing Fixture, 3D Stress Analysis," The MacNeal–Schwendler Corporation, 1987.
10. Schiermeier, J.E., "Automatic p-Adaptivity in MSC/PROBE Version 5," *MSC 1992 World Users' Conference Proceedings*, The MacNeal–Schwendler Corporation, Los Angeles, 1992.